H^∞ Robust Control Synthesis for a Large Space Structure

Michael G. Safonov, Richard Y. Chiang, and Henryk Flashner
University of Southern California, Los Angeles, California 90089

In a design study involving the use of H^∞ optimal control theory, a six-state control law is generated for a 116-state model of a large flexible space structure. A combination of collocated rate feedback and balanced-stochastic-truncation model reduction techniques is found to lead to a vastly simplified four-state model of the structure. Using a singular-value robustness criterion, the four-state model is proved to be satisfactory for the design of a controller whose bandwidth exceeds the natural frequencies of all of the modes of the original 116-state model. Specifications regarding disturbance attenuation, bandwidth, and stability robustness are quantitatively expressed as weighting functions in a mixed-sensitivity H^∞ optimal control synthesis problem, the solution to which is computed by using the PRO-MATLAB Robust-Control Toolbox.

Introduction

LARGE space structures (LSS) pose a challenging problem in control system design because of the large size, large modeling uncertainty, low rigidity, and low damping that are characteristic of the finite element models usually employed for such designs. Among the techniques that have been used to design controllers for LSS are frequency-weighted linear quadratic Gaussian (LQG),[1] Independent Modal Space Control (IMSC)[2], positivity combined with multivariable characteristic frequency loci,[3,4] and modified linear quadratic regulator (LQR) control.[5] A major issue in applying these techniques is in including typical LSS robustness and sensitivity constraints in the design methodology. Also, the high-order LSS model makes application of these techniques inefficient and often results in high-order controllers. The H^∞ optimal control approach, when combined with an appropriate model order reduction technique, can overcome these difficulties.

Solution of the H^∞ control problem can be achieved using several different approaches, e.g., the now-obsolete methods[4,6-9] and the more recent two-Riccati descriptor-system methods.[10-13] These methods are implemented by the Robust-Control Toolbox software package developed by Chiang and Safonov.[10]

The H^∞ design approach allows the control analyst to precisely shape the frequency response characteristics according to the performance specifications. Yet, in marked contrast to other design techniques, the H^∞ procedure is extremely simple. One needs only to specify the plant model and performance

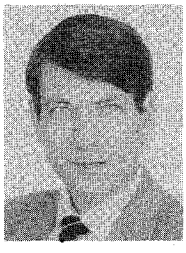

Michael G. Safonov received B.S., M.S., Engineer, and Ph.D. degrees in Electrical Engineering from the Massachusetts Institute of Technology. From 1972 to 1975 he served with the U.S. Navy as an officer aboard an aircraft carrier. Since 1977 he has been with the University of Southern California, where he is presently a Professor of Electrical Engineering and Associate Department Chairman in the Department of Electrical Engineering Systems. He has been a consultant to numerous companies and has authored or coauthored more than 100 publications. He is a Senior Member of the AIAA and a Fellow of the IEEE.

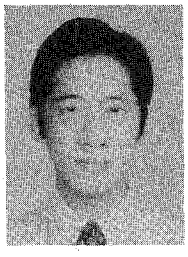

Richard Y. Chiang received a Ph.D. in Electrical Engineering from the University of Southern California, Los Angeles, in 1988. Since 1989 he has been with the the Control Systems Research Group at Northrop Aircraft as an Engineering Specialist, and he teaches part time at the University of Southern California. From 1976 to 1985 he worked full time for various aerospace companies (CTCI, AiResearch, and Lear Astronics) as a control systems analyst. His research interests include robust control, H^∞ optimal control theory, model reduction, and their application to aerospace systems. He is coauthor with M. G. Safonov of the software package *Robust-Control Toolbox* (MathWorks, 1988). His current mailing address is at the Flight Control and Research Group, Northrop Aircraft, Hawthorne, CA 90250.

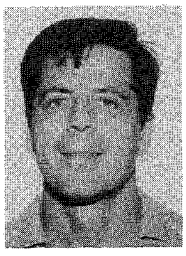

Henryk Flashner is an Associate Professor of Mechanical Engineering at the University of Southern California in Los Angeles. He earned his B.S. and M.S. degrees from Technion-Israel Institute of Technology in 1971 and 1974, respectively, and a Ph.D. from the University of California, Berkeley in 1979. From 1979 to 1983 he was a Member of the Technical Staff in the Control Engineering Department at TRW Space Technology Group, Redondo Beach, CA. His research interests include control of flexible mechanical systems, attitude control of spacecraft, and analysis of nonlinear dynamical systems. He is a member of AIAA.

Received July 11, 1989; revision received Feb. 15, 1990; accepted for publication July 10, 1990.

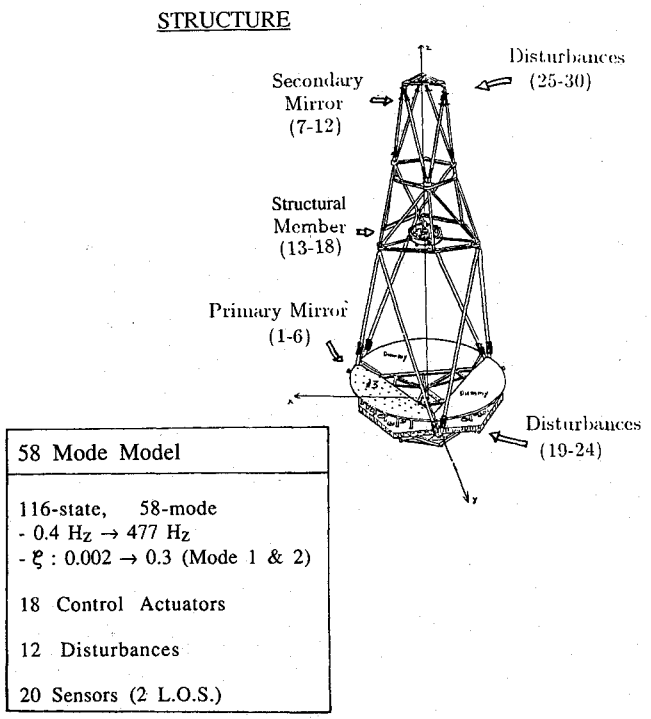

Fig. 1 Large space structure.

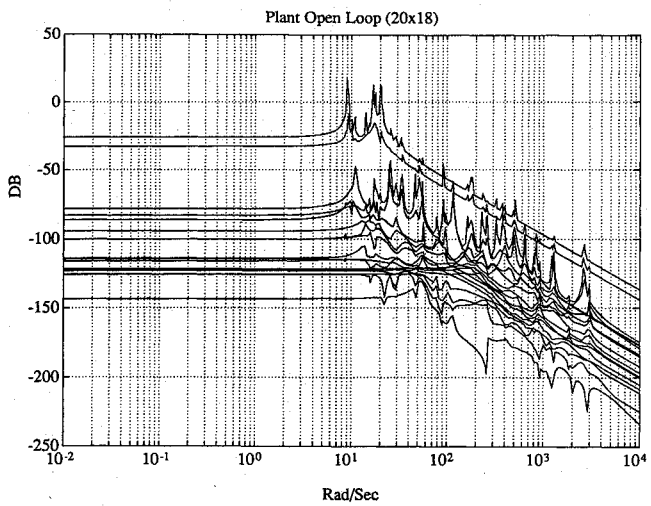

Fig. 2 Singular-value Bode plot of LSS open loop.

and robustness specifications in the form of weighting functions and then an H^∞ software package, such as the Robust-Control Toolbox, can automatically compute an H^∞ controller. In this paper, the H^∞ design method is used to design a controller for active attenuation of structural vibrations in a large flexible space structure. The control design objective is to achieve at least 100:1 reduction in line of sight (LOS) error with respect to open-loop performance in the presence of disturbances over the frequency range of 1-15 Hz.

The controller design in this paper was obtained via the following four steps: 1) collocated rate feedback to damp important modes and facilitate model reduction; 2) squaring-down compensation, which selects suitable linear combinations of control actuators; 3) model reduction of a 116-state model to a four-state model using the Schur balanced stochastic truncation (BST) algorithm[14]; and 4) H^∞ optimal feedback. The four-step design strategy and the issue of robustness, pertinent to both H^∞ and model reduction, are discussed in detail in the remainder of this paper.

The complete design work was carried out using the Robust-Control Toolbox and PRO-MATLAB on a SUN 3/50 workstation.

Plant Description and Design Specifications

In this section, we describe the mathematical model of the plant and the control system design specification.

Plant Description

The LSS model was generated using the NASTRAN finite element program by TRW Space Technology Group. It consists of 58 vibrational modes with frequencies ranging from 0.4 to 477 Hz. The damping ratio is 0.3 for the first two modes and 0.002 for the rest of the modes. The first two modes correspond to rigid-body tilt about the x and y axes; the heavy damping of these modes results from mechanical dampers through which the structure is attached to a massive base. The structure is controlled by 18 actuators commanded by one central computer with a sampling frequency of 3000 Hz. The actuators are grouped in three locations: six are at the primary mirror, six at the secondary mirror, and six on structural members, as shown in Fig. 1. Twelve disturbances are acting on the top and bottom of the structure to simulate the real enviromental vibration source. There are 20 sensors located at various locations in the structure. The most important sensors are the two LOS position sensors. The remaining 18 sensors measure rate of change of position and are collocated with the 18 control actuators. Figure 2 shows a singular value Bode plot of the plant open-loop transfer function matrix from the 18 control actuators to the 20 sensors.

A state-space representation of the open-loop plant is

$$\dot{x} = Ax + Bu \tag{1}$$

$$y = Cx \tag{2}$$

where $A \in \mathbb{R}^{116\times116}$, $B \in \mathbb{R}^{116\times30}$, and $C \in \mathbb{R}^{20\times116}$.

The complete state-space model can be found in Safonov et al.[15] The theory of structural dynamics can be found in Clough.[16]

Design Specifications

The LSS design specification requires the LOS error to be attenuated from an open-loop root-mean-square (rms) value of about 20,000 μrad to not more than 200 μrad after the feedback control loops are closed. The power spectrum of open-loop error signal is contained in the frequency range 0-15 Hz. Thus, we need to design a controller for the LSS such that the two LOS errors are attenuated 100:1 for disturbances whose power spectrum lies within this frequency range. Allowing for a 30-dB/decade rolloff beyond 15 Hz places the control loop bandwidth at roughly 300 Hz ($\approx$2000 rad/s). In terms of inequalities to be satisfied by the open-loop singular value Bode plot, these specifications are as depicted in Fig. 3.

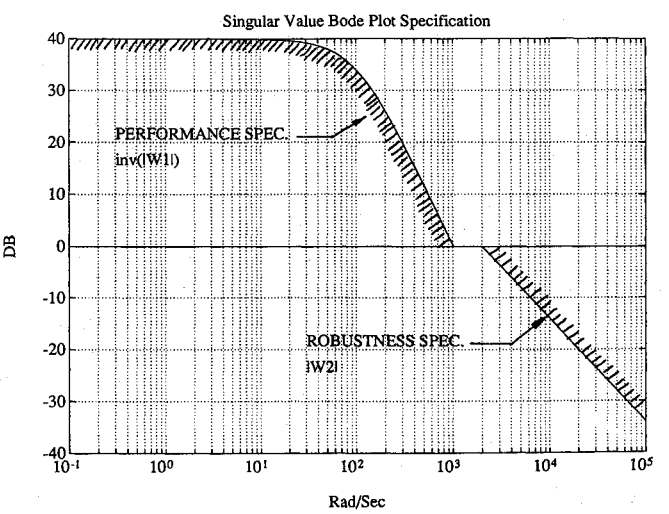

Fig. 3 LSS singular-value specification.

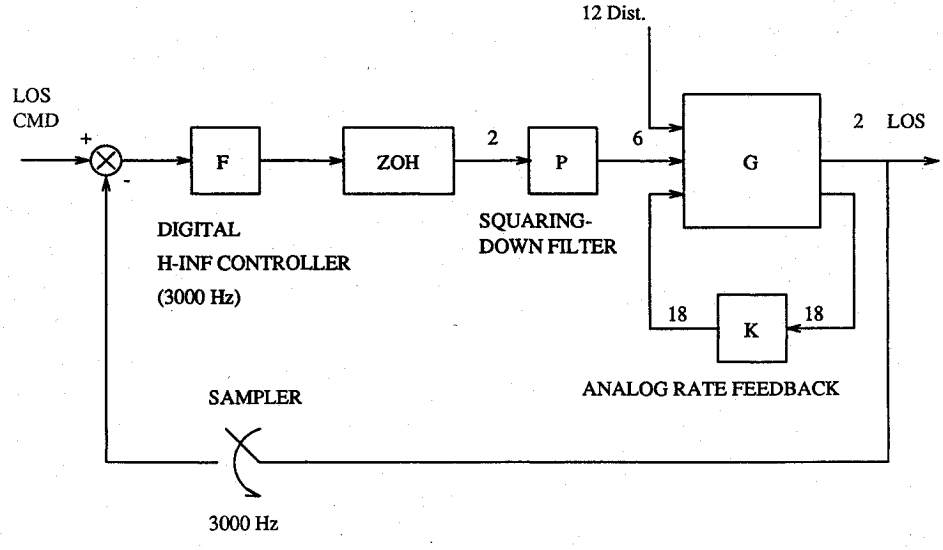

Fig. 4 Digital H^∞ controller block diagram.

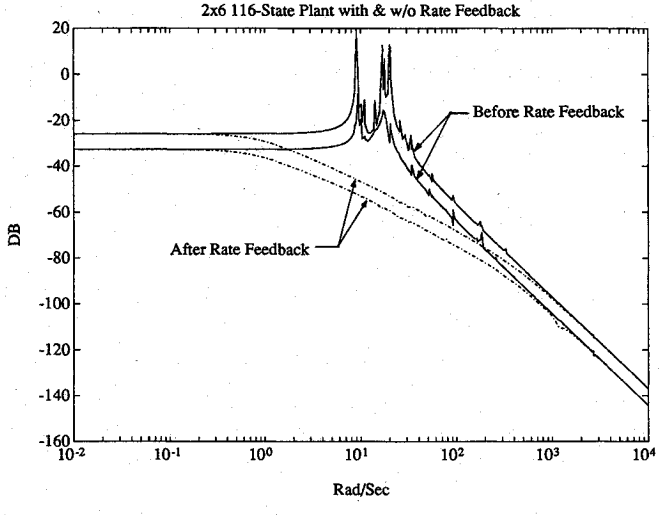

Fig. 5 Plant open loop: six mirror actuators to two LOS sensors (before and after rate feedback).

Together with H^∞, we choose singular values as our design tool. Singular values quantify the robustness, sensitivity, and disturbance rejection of a system.[17]

Control Actions

Our design strategy for the LSS's LOS loops is as follows (see Fig. 4):

1) Use the 18 collocated rate feedback loops to damp some of the structural modes (inner loops), to facilitate model reduction and to make it possible to use the six primary mirror actuators to control the two LOS outputs (outer loops).

2) Square down the plant to a 2×2 transfer function matrix by selecting two linear combinations of actuators that are effective for controlling the two LOS outputs.

3) Find a reduced-order model of the 116-state plant with collocated rate feedback loops closed.

4) Use the H^∞ control design method to push down the sensitivity in order to achieve the requisite 100:1 disturbance attenuation over the frequency range 0–15 Hz.

We will discuss each design phase in the following sections.

Collocated Rate Feedback

Using collocated rate feedback to damp a passive structure is the easiest and least expensive control approach.[18] Collocated rate feedback is robust; it can never destabilize a passive structure due to its passivity characteristics,[19] provided actuator and sensor phase lag is smaller than ± 90 deg inside the rate-feedback control-loop bandwidths. That is, it guarantees a phase margin of at least ± 90 deg in every feedback loop even when the phase variations occur simultaneously in all loops. In addition, rate feedback simplifies the input-output relation of the system, tending to drive some lightly damped poles toward zeros, thereby allowing more effective model reduction in later stages of the design. When the rate loops are closed with proper gains, poles tend to move further to the left in the complex plane or move toward lightly damped open-loop zeros. Those modes that approach open-loop zeros become nearly decoupled in an input-output sense from the sensors and/or actuators in the rate loops. The resulting model can then be reduced using more advanced model reduction techniques such as Hankel MDA,[20] Schur balanced truncation,[21] or Schur BST[14]; software implementations are available as functions in the Robust-Control Toolbox.[10] Once a reasonably sized model is obtained, the H^∞ control design method can be applied to obtain a controller of order comparable to that of the reduced plant model.[22]

After the collocated rate feedback loops are closed, the state dynamics become

$$\dot{x} = (A - B_{18}KC_{18})x \tag{3}$$

where B_{18} consists of the first 18 columns of B (corresponding to the 18 control actuator inputs)

$$B_{18} := \text{(18 control actuators)}$$

and C_{18} consists of rows 3–20 of C; in our case,

$$C_{18} := B_{18}^T \quad \text{(collocated rate sensors)}$$

The collocated rate feedback gain chosen was

$$K = \text{diag}(K_1, K_2, K_3)$$

where $K_1 = 5000I_6$ for primary mirror actuators, $K_2 = 10{,}000I_6$ for secondary mirror actuators, $K_3 = 20{,}000I_6$ for structure member actuators, and I_6 denotes the 6×6 identity matrix. This set of gains was selected based on trial and error.[15]

The singular value Bode plots of the 2×6 transfer function matrix from the six primary mirror actuators to the two LOS sensors are shown in Fig. 5, both before and after the rate loops are closed. As may be seen from Fig. 5, the singular-value Bode plots after rate feedback lose the jagged peaks and valleys as some poles become better damped and others move toward lightly damped zeros when the rate-feedback loops are closed. This smoothing of the Bode plots greatly facilitates

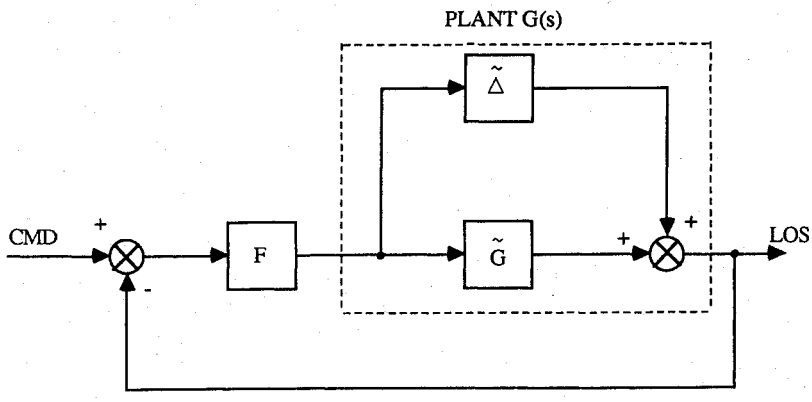

Fig. 6 Plant uncertainty.

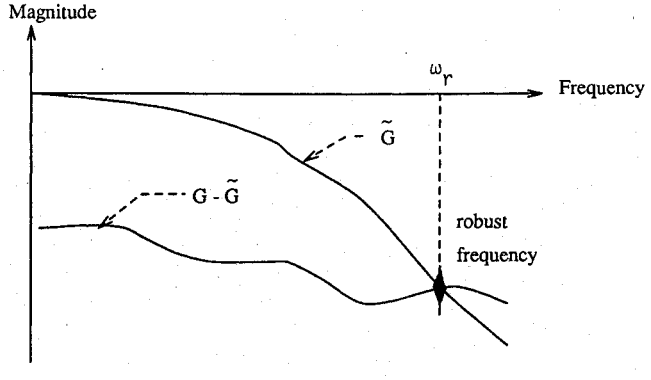

Fig. 7 Robust frequency. (A reduced-model $\tilde{G}$ is valid for control designs having bandwidth up to the robust frequency ω_r.)

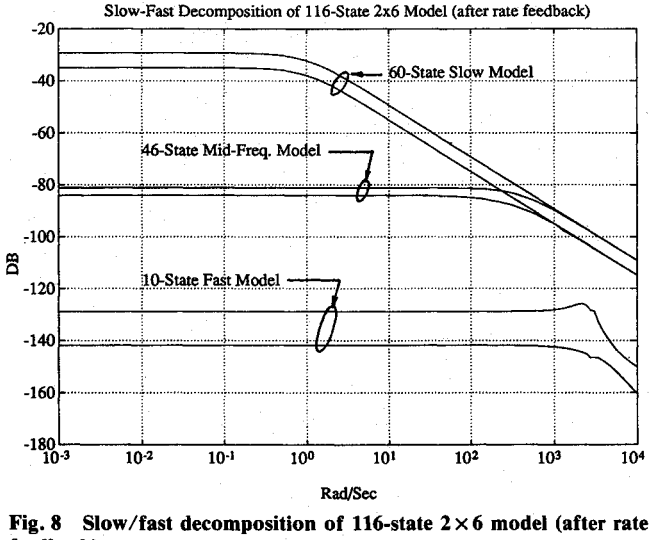

Fig. 8 Slow/fast decomposition of 116-state 2×6 model (after rate feedback).

matching the frequency response data with a simplified reduced order model.

Squaring Down and Model Reduction

Robustness Issue

Before attempting model reduction, we must address the question, "How accurate must a reduced model be in order to be reliably used?" Singular-value Bode plots of a reduced plant model and the modeling error provide the information needed to answer this question.

Let $G(s)$, $\tilde{G}(s) \in C^{n\times n}$ be a true plant transfer function matrix and its reduced model, respectively. Then, the additive modeling error is defined as (see Fig. 6)

$$\tilde{\Delta} := G - \tilde{G}$$

The following theorem and definition quantify the tolerable size of $\tilde{\Delta}$ in terms of singular values and establish a relationship with the achievable control-loop bandwidth. In the following, $\underline{\sigma}$ and $\bar{\sigma}$ denote the minimum and the maximum singular value, respectively.

Theorem 1. Consider the system shown in Fig. 6. Suppose that the perturbation $\tilde{\Delta}$ has no unstable poles and that the feedback F stabilizes the nominal plant $\tilde{G}$. If for all frequency ω

$$\frac{\bar{\sigma}(\tilde{\Delta})}{\underline{\sigma}(\tilde{G})}\,\bar{\sigma}\left[\tilde{G}F(I+\tilde{G}F)^{-1}\right] < 1 \tag{4}$$

then F stabilizes the perturbed plant G.

Proof. See, for example, Chiang and Safonov.[10]

Definition 1 (see Fig. 7). Given G, $\tilde{G}$, and $\tilde{\Delta}$ as noted earlier, the robust frequency is

$$\omega_r := \max\left\{\omega \,|\, \underline{\sigma}\left[\tilde{G}(j\omega)\right] \geq \bar{\sigma}\left[\tilde{\Delta}(j\omega)\right]\right\}$$

The significance of the robust frequency in the context of model reduction is that the robust frequency ω_r is an upper bound on the bandwidth of any multivariable control system that can be designed without violating the sufficient condition for stability [Eq. (4)] at some frequency within the bandwidth. Loosely speaking, the bandwidth ω_B of a control system is the frequency range where the loop transfer function is large, i.e.,

$$\underline{\sigma}(\tilde{G}F) \gg 1 \qquad \text{for all } \omega < \omega_B \tag{5}$$

Notice that for $\omega < \omega_B$ where Eq. (5) is satisfied one has

$$\bar{\sigma}\left[\tilde{G}F(I+\tilde{G}F)^{-1}\right] \approx 1 \tag{6}$$

and, hence, Eq. (4) becomes approximately $\bar{\sigma}(\tilde{\Delta}) < \underline{\sigma}(\tilde{G})$. Thus, one has the following robustness criterion[23]:

If $\bar{\sigma}(\tilde{\Delta}) \leq \underline{\sigma}(\tilde{G})$ for $\omega \leq \omega_r$ (with $\tilde{\Delta}$ and $\tilde{G}$ open-loop stable), then the closed-loop system will be stable provided that the control bandwidth is less than the robust frequency ω_r. (This is only sufficient, not necessary.)

The implication is that to achieve the bandwidth of 300 Hz ($\approx$2000 rad/s) specified for the LSS, it should suffice to use any reduced model having robust frequency $\omega_r > 2000$ rad/s.

Note that our robustness criterion requires that $\tilde{G}$ be square since $\underline{\sigma}$ is only defined for square matrices; this assumption cannot be relaxed. Accordingly, the 2-output-6-input LSS plant must be squared down with a suitable 6×2 pre-compensator before we can apply the robustness criterion. Note, however, that if the squaring-down precompensator were the pseudoinverse of the plant, then one may easily show that the ω_r computed from Definition 1 before squaring down would necessarily be at least as great as that obtained after squaring down. In practice, of course, pseudoinverse precompensation usually cannot be exactly realized without unstable pole-zero

cancellation, but we may use a constant approximation of it. More sophisticated methods for computing squaring-down compensators are described by Le and Safonov.[24]

Squaring-Down Compensator Design

The LSS transfer function matrix from its six primary actuators to its two LOS sensors after collocated rate loops are closed can be decomposed as follows (the complete model with all mode frequencies after rate feedback is listed in Safonov et al.[25]):

$$G = G_s + G_m + G_f \tag{7}$$

where G_s has the slow modes (60 states), G_m the midfrequency modes (46 states), and G_f the fast modes (10 states). The singular-value Bode plots are shown in Fig. 8.

Clearly, $\bar{\sigma}(G_f) \ll \underline{\sigma}(G_s + G_m)$, and so it follows from the robustness criterion that G_f may be discarded from the model. Furthermore, the corner at $\omega = 10$ rad/s and the first order 20-dB/decade rolloff of the Bode plots of G_s suggest that it may be possible to model G_s as

$$G_s(s) := C_s(Is - As)^{-1}B_s \approx \left[1/(s+1)\right] C_s B_s$$

Choosing the precompensator P to be the pseudoinverse of $C_s B_s$

$$P := (C_s B_s)^{\dagger}$$

yields

$$G_s P \approx \begin{bmatrix} 1/(s+1) & 0 \\ 0 & 1/(s+1) \end{bmatrix}$$

A singular-value Bode plot of this two-state reduced model $G_s P$ and the error $GP - G_s P$ is shown in Fig. 9. The plot shows the robust frequency to be at $\omega_r = 800$ rad/s; this is too low for the specified 2000 rad/s control bandwidth. A more sophisticated model reduction procedure was required to identify a reduced-order model with the requisite robust frequency of 2000 rad/s or greater.

We were able to achieve the desired robust frequency using the Schur BST model reduction algorithm.[10,14] However, a slight modification to the Schur BST procedure was required because BST requires that the model being reduced be full rank at frequency infinity. In our case, the model being reduced $G(s)P$ is zero at frequency infinity. To overcome this problem, we added a small rank-two constant matrix D to $G(s)P$, taking care that $\bar{\sigma}(D) < \underline{\sigma}[G(j\omega)]$ for all ω in the proposed control bandwidth, i.e., $\omega \leq 2000$ rad/s. We then applied Safonov and Chiang's Schur BST procedure[10,14] to the augmented model $G(s)P + D$ and subtracted D from the resulting reduced model to obtain a four-state model that is zero at frequency infinity. The singular value Bode plots in Fig. 10 indicate that the four-state reduced model thus obtained has a robust frequency $\omega_r = 2 \times 10^6$ rad/s, well above the specified 2000-rad/s LOS control-loop bandwidth.

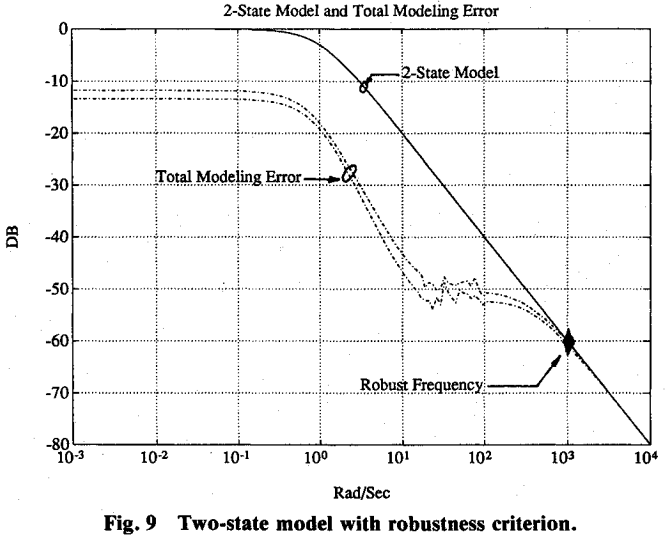

Fig. 9 Two-state model with robustness criterion.

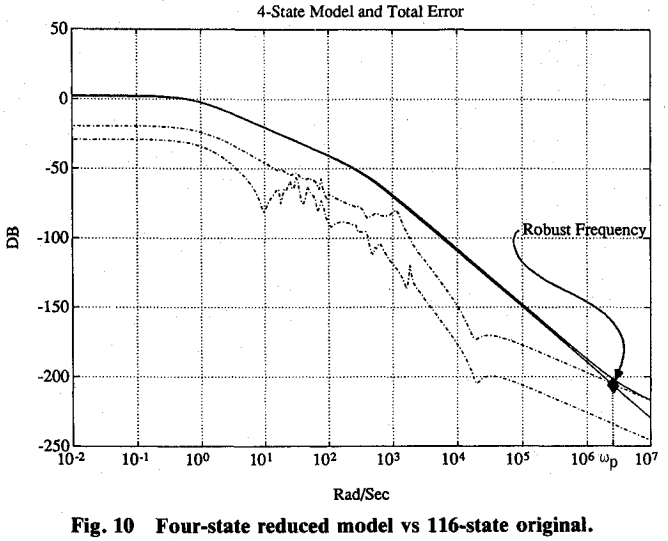

Fig. 10 Four-state reduced model vs 116-state original.

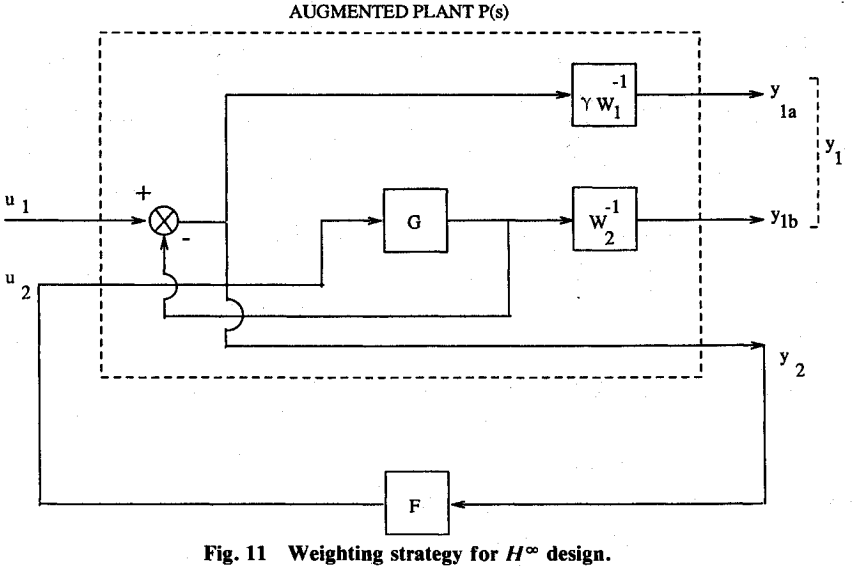

Fig. 11 Weighting strategy for H^{∞} design.

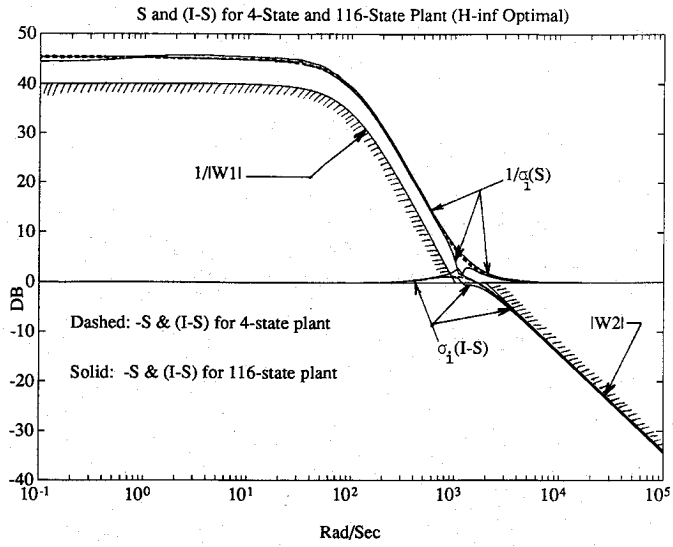

Fig. 12 H^∞ design results.

This four-state model (listed in Appendix A) is ready for outer-loop H^∞ optimal control design.

H^∞ Controller Design

In this section, we describe how we applied the H^∞ optimal control theory to the two-input-two-output four-state reduced model $\tilde{G}(s)$ of the squared-down LSS with rate feedback. An H^∞ optimal control design results in a controller having degree $n-1$ (or less) where n is the combined degree of the plant and weights.[22] Thus, the model reduction performed in the previous design step was essential to ensure that the degree of the H^∞ controller would be acceptably small. For further background on the state-space H^∞ theory, see Refs. 11–13 and 26, wherein additional references may be found.

We begin by describing how we transformed the LSS design specifications into the two-block mixed-sensitivity H^∞ problem framework exactly as was previously done for the aircraft example of Safonov and Chiang.[26] For the LSS, we represent the performance and robustness specifications by the weighted mixed-sensitivity H^∞ inequality

$$\|T_{y_1u_1}\|_\infty \le 1$$

where

$$T_{y_1u_1} := \begin{bmatrix} \gamma W_1^{-1} S \\ W_2^{-1}(I-S) \end{bmatrix}$$

$$S := (I+\tilde{G}F)^{-1}$$

$W_1(s)$ and $W_2(s)$ are frequency-dependent weighting functions, and $\gamma > 0$ is a design parameter. The weights W_1 and W_2 are chosen to reflect the robustness and bandwidth requirements, viz. 100:1 disturbance attenuation and 2000-rad/s bandwidth (see Fig. 11).

The selected weights are given in Appendix A and Bode plots of $1/|W_1|$ and $|W_2|$ are shown in Fig. 12. Note that the 0-dB crossover frequency for $|W_2|$ is chosen to be precisely the desired maximum closed-loop bandwidth of 2000 rad/s. The real parameter γ is used as a design knob that is iteratively increased until our H^∞ software package informs us that the inequality $\|T_{y_1u_1}\|_\infty \le 1$ can no longer be satisfied.

The augmented plant $P(s)$ is the only input data to the Robust-Control Toolbox software program. The iteration on γ proceeds as follows: If there exists a stabilizing controller F for which $\sup\bar{\sigma}(T_{y_1u_1}) \le 1$, then the program finds one such H^∞ controller. We iteratively increase the coefficient γ of W_1^{-1} until the singular values of S and $(I-S)$ are pushed against their limits $\gamma^{-1}W_1$ and W_2; the singular-value Bode plots then assume the shape of the Bode plots of $|\gamma^{-1}W_1(j\omega)|$ and $|W_2(j\omega)|$ as a consequence of the all-pass property that is characteristic of all H^∞ optimal control systems (e.g., Francis[6] and Safonov et al.[8]). If we were to increase γ too far, this would result in either closed-loop instability or the $\sup\bar{\sigma}(T_{y_1u_1}) > 1$. In the present case, the optimal γ is found after several iterations to be $\gamma = 1.78125$. The singular-value Bode plots of S and $I-S$ for this value of γ are shown in Fig. 12. Clearly, the design specifications have been met completely (actually exceeded).

After the H^∞ design, we connected the H^∞ controller to the 116-state plant and examined the singular-value Bode plots (see Fig. 12). As one would expect based on our robustness criterion, the plots deviate only insignificantly from the four-state plant case.

Finally, the continuous H^∞ control design was discretized for use at a 3000 Hz sampling rate via the s-plane to z-plane conformal map

$$s = 6000\left[\frac{z-1}{1+(z/0.8)}\right] \tag{8}$$

yielding the discrete-time control law given in Appendix B.[15] Note that the state-space realization of the control law given in Appendix B has six states, which agrees with the theoretical prediction[22] of at most $n-1$ for an n-state augmented plant since in this case $n = 8$.

The final optimal H^∞ controller sampled at 3000 Hz and applied to the 116-state linear model achieves the following performance (see block diagram Fig. 4)[15]:

1) 2000 rad/s (318 Hz) bandwidth.

2) 20.682 μrad rms error in LOS (1000:1 reduction), see Fig. 13.

3) At least a 10–12-dB gain margin and more than 50-deg phase margin in each feedback loop.

4) The capability of tolerating at least $\pm 70\%$ plant uncertainty without instability (this follows from the fact that the

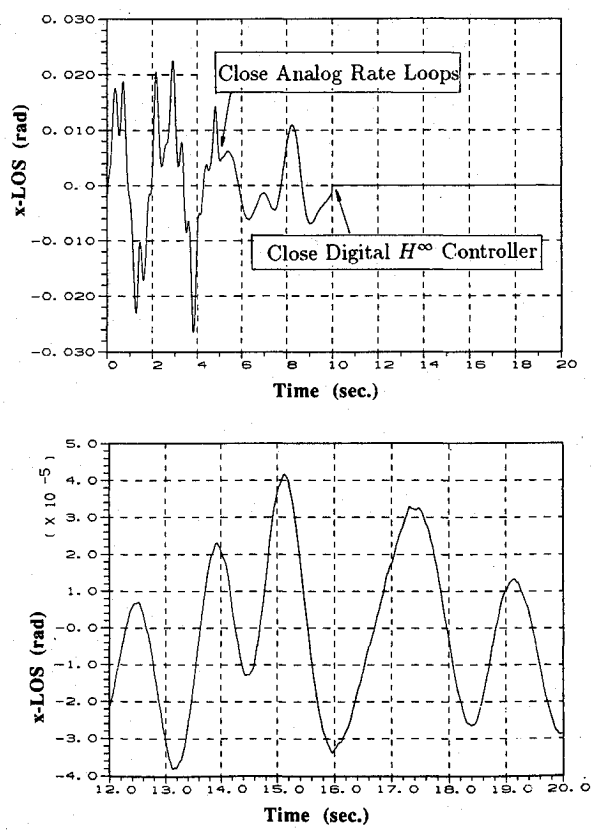

Fig. 13 Simulated LOS time history showing effect of closing analog referenced back loops and the digital H^∞ loops.

closed-loop singular-value Bode plot of the complementary sensitivity is bounded above by 3 dB, see Safonov et al.[17]).

Conclusions

Using a combination of collocated analog rate feedback, Schur balanced-stochastic-truncation (BST) model reduction, and digital H^∞ optimal feedback, a robust multivariable controller has been designed for active vibration suppression for a 116-state model of the large flexible space structure. Using collocated rate feedback to precondition the plant for model reduction and our robustness criterion to quantify the modeling accuracy required to achieve our given disturbance attenuation and control bandwidth objectives, a crude four-state reduced model (which we found via the Schur BST model reduction method) was proven to be adequate throughout the entire bandwidth covered by the modes of the original 116-state model. Specifications for disturbance attenuation, bandwidth, and stability robustness were easily formulated in the framework of a weighted two-block mixed-sensitivity H^∞ optimal control problem. The H^∞ design procedure itself was direct and automated, enabling direct manipulation of disturbance attenuation and robustness tradeoffs.

Appendix A: State Space of the LSS Four-State Model (Squaring-Down Filter Included) and the Weighting Functions

$$\left[\begin{array}{c|c} A & B \\ \hline C & D \end{array}\right] := \left[\begin{array}{rrrr|rr} -1.1938e+02 & 1.8788e+01 & -8.2091e+01 & -1.4185e+00 & 1.3531e+00 & -1.6578e+00 \\ 3.2276e+01 & -1.1417e+01 & 2.2510e+01 & 1.0717e+01 & -8.5719e-02 & 6.3927e-01 \\ -4.0590e+02 & 6.4353e+01 & -2.8176e+02 & -4.8977e+00 & 4.5709e+00 & -5.6314e+00 \\ 2.0075e+01 & 1.8203e+02 & 7.7849e+00 & -3.4213e+02 & -8.3185e+00 & -5.2742e+00 \\ \hline 2.8218e+01 & 1.4678e+01 & -7.1289e+00 & 5.2135e-01 & 0 & 0 \\ -3.8988e+01 & 1.9700e+01 & 1.3101e+01 & 6.5414e-01 & 0 & 0 \end{array}\right]$$

$$W_1 = \frac{1\times10^{-6}s^2+2\times10^{-4}s+1\times10^{-2}}{4\times10^{-8}s^2+4\times10^{-4}s+1} I_2, \qquad W_2 = \frac{2000}{s} I_2$$

where I_2 denotes a 2×2 identity matrix.

Appendix B: State-Space Matrices $\left[\begin{array}{c|c} A & B \\ \hline C & D \end{array}\right]$ of the H^∞ Controller

$$\left[\begin{array}{rrrrrr|rr} -2.3541e+07 & 2.6678e+07 & 1.6391e+08 & -2.1089e+08 & -1.1029e+09 & 2.1272e+08 & 1.4087e+09 & -4.6342e+08 \\ 1.9468e+07 & -2.7699e+07 & -1.7889e+08 & 1.9010e+08 & 1.0930e+09 & -3.2999e+08 & -1.4824e+09 & 3.0814e+08 \\ -1.1965e+04 & 1.7892e+04 & 1.1775e+05 & -1.1925e+05 & -7.0322e+05 & 2.3158e+05 & 9.6773e+05 & -1.7381e+05 \\ 8.1782e+03 & -1.0096e+04 & -6.3310e+04 & 7.6692e+04 & 4.1284e+05 & -9.3792e+04 & -5.3753e+05 & 1.5551e+05 \\ -1.8490e+02 & 2.4863e+02 & 1.7508e+03 & -2.0602e+03 & -1.1240e+04 & 2.7418e+03 & 1.3737e+04 & -3.3966e+03 \\ 1.1637e+01 & -3.7186e+01 & -4.5035e+02 & -4.0294e+01 & 1.3178e+03 & -2.0888e+03 & -2.3484e+03 & -6.1948e+02 \\ \hline -2.5610e+06 & 3.4742e+06 & 2.2230e+07 & -2.4535e+07 & -1.3835e+08 & 3.8778e+07 & 1.8547e+08 & -4.2794e+07 \\ 3.4464e+06 & -3.9075e+06 & -2.4010e+07 & 3.0879e+07 & 1.6152e+08 & -3.1192e+07 & -2.0634e+08 & 6.7819e+07 \end{array}\right]$$

Acknowledgments

This work was supported in part by TRW Space and Technology Group and in part by Air Force Office of Scientific Research Grants 85-0256 and 88-0282. We thank Kevin McLaughlin at TRW Space and Technology Group for testing our digital controller with TRW's large nonlinear time simulation program and successfully verifying our results.

References

[1]Gupta, N., "Frequency-Shaped Cost Functionals: Extension of Linear-Quadratic-Gaussian Design Methods," *Journal of Guidance and Control,* Vol. 3, No. 6, 1980, pp. 529–535.

[2]Meirovitch, L., and Baruch, H., "Control of Self-Adjoint Distributed Parameter System," *Journal of Guidance and Control,* Vol. 5, No. 1, 1982, pp. 60–66.

[3]Sesak, J. R., Likins, W. and Coradetti, T., "Flexible Spacecraft Control by Model Error Sensitivity Suppression," *Proceedings of the Second VPI and SU/AIAA Symposium on Dynamics and Control of Large Flexible Spacecraft,* edited by L. Meirovitch, Engineering Mechanics Dept., Virginia Polytechnic Inst., Blacksburg, VA, 1979.

[4]Benhabib, R. J., and Tung, F. C., "Large-Scale Space Structures Control: System Identification Versus Direct Adaptive Control," *Proceedings of the Joint Automatic Control Conference,* San Francisco, CA, Inst. of Electrical and Electronics Engineers, Piscataway, NJ, Aug. 1980.

[5]Benhabib, R. J., Iwens, R., and Jackson, K. L., "Stability of Distributed Control for Large Flexible Structures Using Positivity Concepts," *Journal of Guidance and Control,* Vol. 4, No. 5, 1981, pp. 487–494.

[6]Francis, B. A., *A Course in H^∞ Control Theory,* Springer-Verlag, New York, 1987.

[7]Kwakernaak, H., "A Polynomial Approach to Minimax Frequency Domain Optimization of Multivariable Feedback Synthesis," *International Journal of Control,* Vol. 44, No. 1, 1986, pp. 117–156.

[8]Safonov, M. G., Jonckheere, E. A., Verma, M., and Limebeer, D. J. N., "Synthesis of Positive Real Multivariable Feedback Systems," *International Journal of Control,* Vol. 45, No. 3, 1987, pp. 817–842.

[9]Chiang, R. Y., and Safonov, M. G., "The LINF Computer Program for L^∞ Controller Design," Dept. of EE-Systems, Univ. of Southern California, Los Angeles, CA, EECG-0785-1, Version 2.0, July 1987.

[10]Chiang, R. Y., and Safonov, M. G., *Robust-Control Toolbox,* MathWorks, South Natick, MA, 1988.

[11]Glover, K., and Doyle, J. C., "State Space Formulae for All Stabilizing Controllers that Satisfy an H_∞-Norm Bound and Relations to Risk Sensitivity," *Systems and Control Letters,* Vol. 11, No. 3, 1988, pp. 167–172.

[12]Safonov, M. G., and Limebeer, D. J. N., "Simplifying the H^∞ Theory via Loop Shifting," *Proceedings of the IEEE Conference on Decision and Control,* Austin, TX, Dec. 7–9, 1988, Inst. of Electrical

and Electronics Engineers, Piscataway, NJ, 1988.

[13]Safonov, M. G., Limebeer, D. J. N., and Chiang, R. Y., "Simplifying the H^∞ Theory via Loop-Shifting, Matrix Pencil and Descriptor Concepts," *International Journal of Control,* Vol. 50, No. 6, 1989, pp. 2467–2488.

[14]Safonov, M. G., and Chiang, R. Y., "Model Reduction for Robust Control: A Schur Relative Error Method," *International Journal of Adaptive Control and Signal Processing,* Vol. 2, 1988, pp. 259–272.

[15]Safonov, M. G., Chiang, R. Y., and Flashner, H., "USC Large Space Structure Control Design—Final Report," TRW Space and Technology Group, Redondo Beach, CA, July 1987.

[16]Clough, R. W., *Dynamics of Structures,* McGraw-Hill, New York, 1975, Chap. 11–13.

[17]Safonov, M. G., Laub, A. J., and Hartmann, G. L., "Feedback Properties of Multivariable Systems: The Role and Use of Return Difference Matrix," *IEEE Transactions on Automatic Control,* Vol. AC-26, No. 1, 1981, pp. 47–65.

[18]Martin, G. D., "On the Control of Flexible Mechanical Systems," Ph.D. Dissertation, Stanford Univ., Stanford, CA, Aug. 1978.

[19]Zames, G., "On the Input-Output Stability of Time-Varying Nonlinear Feedback Systems," *IEEE Transactions on Automatic Control,* Vol. AC-11, Nos. 2 and 3, 1966, pp. 228–238, 465–476.

[20]Safonov, M. G., Chiang, R. Y., and Limebeer, D. J. N., "Optimal Hankel Model Reduction for Nominal Systems," *IEEE Transactions on Automatic Control,* Vol. AC-35, No. 4, 1990, pp. 496–505.

[21]Safonov, M. G., and Chiang, R. Y., "A Schur Method for Balanced-Truncation Model Reduction," *IEEE Transactions on Automatic Control,* Vol. AC-34, No. 7, 1989, pp. 729–733.

[22]Limebeer, D. J. N., and Halikias, G. D., "A Controller Degree Bound for H^∞ Optimal Control Problems of the Second Kind," *Journal of Control,* Vol. 26, No. 3, 1988, pp. 646–677.

[23]Safonov, M. G., "Frequency Response Methods for Multivariable Control," *Short Course Lecture Notes,* AIAA, Long Beach, CA, May 1985.

[24]Le, V. X., and Safonov, M. G., "Rational Matrix GCD's and the Design of Squaring-Down Compensators—A State Space Theory," *IEEE Transactions on Automatic Control* (to be published).

[25]Safonov, M. G., Chiang, R. Y., and Flashner, H., "H^∞ Control Synthesis for a Large Space Structure," *Proceedings of the American Control Conference,* Atlanta, GA, June 1988, Inst. of Electrical and Electronics Engineers, Piscataway, NJ, 1988.

[26]Safonov, M. G., and Chiang, R. Y., "CACSD Using the State-Space L^∞ Theory—A Design Example," *IEEE Transactions on Automatic Control,* Vol. AC-33, No. 5, 1988, pp. 477–479.